Energy Conservation of Smart Grid System Using Voltage Reduction Technique and Its Challenges

M. Motinur Rahman
Institute of Electronics, Atomic Energy Research Establishment, Bangladesh Atomic Energy Commission

Saha, Subrata
Institute of Electronics, Atomic Energy Research Establishment, Bangladesh Atomic Energy Commission

M. Z. H. Majumder
Institute of Electronics, Atomic Energy Research Establishment, Bangladesh Atomic Energy Commission

T. Tamrin Suki
Dept. of Science & Humanities, Military Institute of Science and Technology

他

https://doi.org/10.5109/6622879

Energy Conservation of Smart Grid System Using Voltage Reduction Technique and Its Challenges

M. Motinur Rahman[1,2], Subrata Saha[1,2], M. Z. H. Majumder[1,2], T. Tamrin Suki[3], M. Habibur Rahman[2], Fahmida Akter[1], M. A. S. Haque[1], M. Khalid Hossain[1,*]

[1]Institute of Electronics, Atomic Energy Research Establishment, Bangladesh Atomic Energy Commission, Savar, Dhaka 1349, Bangladesh

[2]Department of Electrical and Electronic Engineering, University of Dhaka, Dhaka 1000, Bangladesh

[3]Dept. of Science & Humanities, Military Institute of Science and Technology, Dhaka 1216, Bangladesh.

*Author to whom correspondence should be addressed:
E-mails: *khalid.baec@gmail.com, khalid@kyudai.jp

Abstract: Energy conservation has become crucial due to the present energy crisis in the world. To resolve such crises and reduce peak hours' electricity demand, the conservation voltage reduction (CVR) technique is frequently implemented in the power grid system. In this paper, experimental work along with simulation has been done to conserve energy by employing the CVR technique in a smart grid (SG). To verify the simulation result, an Arduino-based SG has been designed with a real-time clock (RTC) and Wi-Fi module esp8266. A program has been developed and burnt into a microcontroller integrated circuit (IC) of an Arduino board that senses day-to-day peak and/or off-peak hours of electricity consumption. The intelligent program that has been put in the system to control the switching of triode for AC (i.e., TRIAC) with an optocoupler to vary the firing angle α (0-π). At peak hours the developed system optimizes the output supplied voltage to load and it results in lesser supplied power at load. The energy consumption data is then sent to the ThingSpeak cloud for remote monitoring. Data aggregation and analytics can be done on ThingSpeak to estimate the energy consumption trend and according to the trend distribution management can notify the generation section for demand management. It has been found that the CVR technique is feasible in RTC-based SG systems which conserves 8.33 % energy by considering 2 ms as an optimized firing delay while the CVR factor = 1. The developed RTC-based SG could be useful in mitigating the present energy crisis in developing countries.

Keywords: smart grid system, energy conservation technique, energy management system, peak-hour management, voltage optimization.

1. Introduction

With the increasing power demand, greenhouse gas emission has increased tremendously and nature is going to state beyond recovery [1–7]. To reduce greenhouse gas researchers around the world are working on various renewable and sustainable energy technologies [6,8] like solar photovoltaics [9,10], solar thermal collectors [11], wind energy systems [12], carbon dioxide-free energy systems [13], and hydrogen energy systems such as fuel cells [14,15] and nuclear fusion reactors [16,17], etc. The above-mentioned systems could mitigate the energy crisis and can help to build a sustainable energy system. But it is necessary to use existing power efficiently. For this SG could be a solution to utilize the existing energy, i.e., the conventional grid power more effectively.

There are several techniques and approaches in SG such as machine learning (ML) [18], artificial intelligence (AI) [19], stochastic dynamic programming (SDP) [20], load estimation [21], internet of things (IoT) [22], blockchain [23], sensor network (SN) [24], heuristic optimization [25], etc.

Several works have been published in the recent past regarding SG. Ahmad et al. worked to identify common issues for smooth energy distribution operations using ML [18]. The work concluded that ML-based automation targeting energy systems could potentially save $273 to $813 billion [18]. To address cyber threats to smart grids, Mohammadpourfard et al. designed a long short-term memory (LSTM) recurrent neural network (RNN) that distinguishes natural SG changes and real-time attacks [26]. The IEEE 14-bus system was used to test the framework's performance, and the results show that the developed

LSTM-based threat detection model can detect the dynamic behaviors of SGs 90% of the time [26].

Furthermore, some works related to power allocation algorithms in SGs have also been reported. Using the penalty function method, Ma et al. transformed the constrained nonlinear programming problem into an unconstrained optimization problem [27]. Finally, they developed a multi-swarm artificial bee colony (MS-ABC) algorithm to optimize relay assignment that can reduce the cost of the utility company [27].

Pamshetti et al. proposed multistage coordinated CVR technology for both offline and online tests [28]. For the day ahead or online scheduling stochastic CVR formulation has been introduced considering uncertainties in power loads, on the other hand, online simulations have been performed for real-time operations. The method was validated considering various issues including substation voltage change and faulty conditions [28].

El-Shahat et al. studied the utilization of the CVR method on Washington EMC's power system and Georgia Transmission Corporation facilities. They investigated different CVR experimental scenarios, CVR data from smart meters, and experimental CVR management data using supervisory control and data acquisition (SCADA). Then a dynamic prediction model was created using Neural Network (NN) and their model showed a 0.22% of error with respect to the real data collected from the environmental modeling center (EMC) facility and national oceanic and atmospheric administration (NOAA) [29].

To evaluate the CVR effects, J. Xu et al. proposed a micro-perturbation-based load-to-voltage (LTV) process identification method. On a specific hardware-in-the-loop testbed, the suggested method was validated using various scenarios. They found the technique is suitable to be implemented in SG for energy-saving [30]. S. Jayaraman et al. presented a plan for energy savings in large industrial plants using CVR. A stacked isolated voltage optimization module was discussed considering the requirements. They validated their proposal using a prototype unit [31].

To our knowledge, based on the available literature, no work used the CVR technique to save energy by employing the RTC clock in SG yet. However, many of them found the CVR technique is a very effective way to handle peak demand as well as save energy. Many of them proposed AI-based SG which is a far cry from implementation in conventional grid systems. Moreover, in the present energy crisis, this system is not well established and is hard to be implemented in developing countries in the middle of an economic crisis. In this regard, the RTC-based SG system comes to the rescue with its simplicity and feasibility.

Therefore, the objective of this present work was to introduce an RTC-based SG which can mitigate power shortage problems at peak-hour using the CVR technique. To achieve the goal a system is developed that can be implemented in the household consumer end to reduce the energy demand in peak-hour. In this work, for the first time, we used an RTC to sense peak and/or off-peak hours and

ZCD to sense voltage level introducing Arduino to address peak-hour demand management as well as energy conservation. ThingSpeak platform has also been introduced within the system to monitor the trend of energy consumption which allows the distributor to implement the CVR technique more effectively. Thus, this work would be beneficial to soothe the present energy crisis in developing countries accelerated by COVID-19. In the present scenario, grid modification is not feasible from the consumer side especially for household consumers and at peak hours and it is a difficult task to manage the consumer demand or shift their demand. Through the system, it would be possible to manage the demand from the consumer side and the system will also notify the consumer about peak hours and will recommend shifting their energy demand at off-peak hours.

In this work, an Arduino Uno-based algorithm is used to optimize energy consumption during peak hours. RTC module provides the time information to the Arduino and it optimizes the load power consumption with the help of Opto-TRIAC circuitry and ZCD. The system determines the voltage level through a ZCD. ZCD performs the task of zero cross detection of line voltage as well as helps to assess the line voltage level using the Analog port A0 port of Arduino Uno. The developed system also can update the seasonally changeable data from RTC. This feature allows the system to introduce smart functionality within the system. The developed SG can also be connected to the LAN using a wifi module and can be monitored from the distribution end via the ThingSpeak cloud. The SG also allows the distribution end to cut off the supply if it goes beyond the normal consumption limit of a consumer automatically by the react app of ThinSpeak. At the same time, a consumer can also be notified by a tweet on his/her wall. The load response characteristics for the power optimization are analyzed using the MSO44 digital oscilloscope and KEW snap clamp meter. The developed algorithm for energy optimization was also simulated using Proteus 8.9. Finally, the steps and challenges in the optimization of load power during peak hours are discussed.

2. Overview of SG using CVR

An SG comes with a justifiable solution for the sustainable development of the world because of its energy-efficient nature. The main producers and consumers in the smart grid are depicted in Fig. 1 [32]. The flow of energy is indicated by the arrows. It improves the utilization efficiency of the power system [33]. An SG is the future of the electric power grid system. Nowadays, an old technique has been reintroduced to a smart grid system to conserve power and peak demand management which is named as CVR technique [34]. This technique is not the new one to conserve power along with peak-demand management capability but becomes the most relevant technology to introduce with the SG. This technique was first introduced after the commercialization of electricity

but at that time energy management was a real challenge because of unknown types of loads and lack of omnidirectional communication as well as the intelligent system nowadays [35] between consumer and distribution feeder. According to the American National Standard (ANSI), the CVR technique can be applied to save electric energy by lowering the voltage at the consumer metering point. This will also help to maintain the peak demand and additional energy losses [36]. CVR is equally relevant for lowering the electricity expenditure over the year as there is an uprising tendency of the unit cost [37].
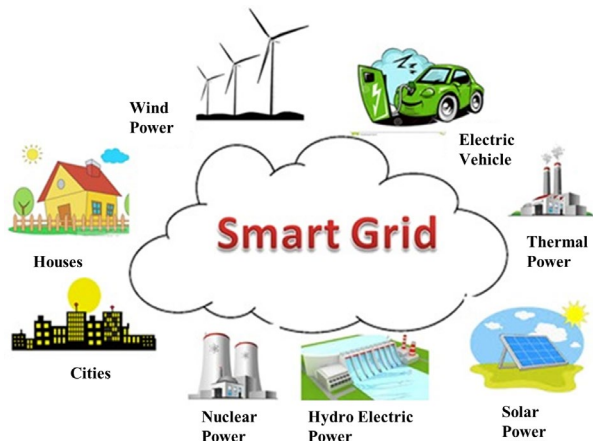

Fig. 1: Main producers and consumers in smart grid. Reproduce with permission from ref. [32]. Copyright 2018 Wiley.

As an emerging technology, the smart grid power system faces many challenges competing with the present power grid system [38]. The primary competition of the conventional grid to SG is the competition of capital. Many investors have invested a lot in conventional grids and it won't be easy to replace them swiftly. Moreover, there is a lack of investors who are readily available to invest in SG-based power systems while there are many investors already playing role in conventional grid-based power systems. Another aspect is the infrastructure development which requires immense development to establish the SG system which will offer secure as well as low-cost energy instead of unreliable, unsecured conventional grid energy. Above all SG system is also facing some challenges from politics, as they are not ready to adapt their energy policy to make a welcoming path for an SG-based power system. However, SG is the instrument available to fight back against climate change by promoting renewable energy sources via its integration and optimal use [39].

On the other hand, conventional grids are less efficient and cause huge system loss and yields frequent blackout throughout the years. It results in high surge voltage that frequently damages electronic and electric equipment. Above all the cost of electricity is rising and there is a rising trend found in the unit cost of electricity. Another weakness of the conventional grid is its vulnerability which is found in many studies [40,41]. But there are also some technical difficulties with immense interdisciplinary

research as SG is still evolving, the SG introduces a duplex communication system between the power consumer and the power grid [42] because of its requirement for bidirectional communication. It controls the grid both from the supplier end to the consumer end. In the SG system, there will be a close connection from the generation end to the consumer end which requires a revolutionary change in transmission, generation and distribution end. But this change is very challenging because many of the steps are still being controlled manually in most of the developing countries. Moreover, there will be a chance of security breach in the communication channel and there is still no established protocol available to acknowledge such type of risk [43–45].

A flatter supply-demand curve will develop as the power grid learns the consumer's consuming habits. This system also provides better efficiency by modifying the supply and demand curve involving programmable logic controller (PLC) and algorithm to control the distribution of power to provide increased power grid distribution efficiency [46].

The consumer end will learn the supply behavior and faults of the power grid. A smart power grid system also introduces clean energy like solar and wind with the power grid system, and power flows bidirectionally. It promotes clean energy with the grid along with promoting the efficiency of conventional fossil fuels [33]. The main challenge of the smart power grid system is the initial cost of integrating it with the conventional power grid system [47]. Demand-side management using an SG requires smart meters along with a LAN connection among them [48] though the SG meters are going to be part of IoT because of the wide availability and cheap cost of LAN connection. Moreover LAN connection is well established where IoT is an emerging technology and it might take few decades to compete and replace LAN [48,49]. Smart load is also important to accommodate the SG. The main feature of the SG is its conservation of power and reduced system loss by combining the latest technology with the conventional grid system [50]. Reducing system loss and conserving power is still a challenge of the grid system that is haunting scientists for a century [51].

3. Methodology

The basic theory of the system is simple, if the supplied voltage to the load is reduced by 2-3 %, the power consumption by the load will be reduced to some extent (typically 1-2%) depending on the load. For instance, according to the 'ZIP' (impedance (Z), current (I), power (P)), model energy consumed by the reactive load with a constant current will consume less power as its power is proportional to the supplied voltage [35,52]. The relationship between voltage reduction and energy conservation can be defined by the factor called 'conservation voltage reduction factor (CVR_f)'.

$$CVR_f = \frac{\% \ Reduction \ of \ Quantities}{\% \ Voltage \ Reduction}$$

Based on the load combination, CVR_f ranges from 0 to 2. To get the exact assessment accurate modeling is required which is beyond the scope of the paper [53,54]. However, there is a rule of thumb determining this factor which states that a 1% voltage reduction saves 1% of power and 1% of peak demand. [55]. A daily load curve shown in Fig. 2 makes it simple to understand energy conservation.
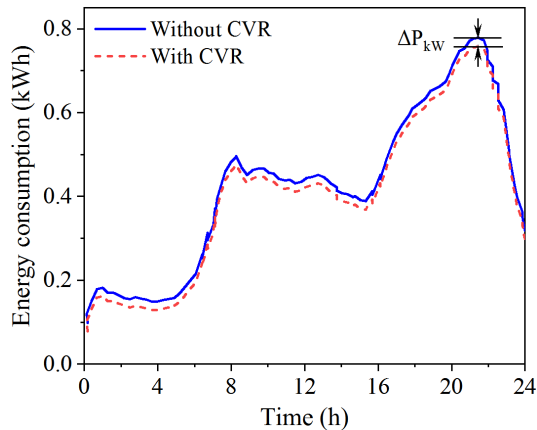

Fig. 2: 24-hour load curve [35].

3.1 Connection protocol of SG to ThingSpeak cloud through LAN

By using software serial, esp8266 is connected to the Arduino Uno digital pins 8, and 10. The digital pin 9 is used for enabling the esp8266 chip. The SG is connected to the LAN through the SSID *NAME* and *PASSWORD*. A channel ID is created on the ThingSpeak cloud where fields are created per consumer. The consumer energy consumption (W) is sent to the cloud using the application programming interface (API) key, IP address, channel ID, and field ID (Fig. 3).
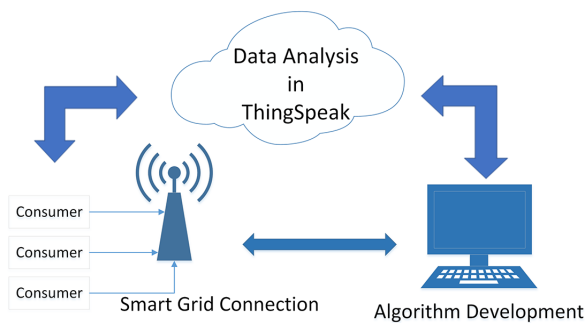

Fig. 3: Control management of SG system.

3.2 ThingSpeak react protocol

First, a react app is created with react name and then a condition was set for a certain channel ID and field. To send a notification of reaction, the consumer's Twitter account is linked with his electricity consumer account

from the distribution end. An action named Thinghttp is also set to send control requests from the distribution end. If the consumer's electricity consumption goes beyond a certain value, developed SG cuts the power line from the distribution end, and a Twitter notification is sent to the consumer.

3.3 System design

Proteus 8.9 is used to simulate all the necessary modules and components for the development and analysis of an SG. Fig. 4 displays a conceptual building block of the developed system. A program has been developed using Arduino IDE and the hex file generated from this platform has been put into the Arduino module of Proteus. All the modules and components are connected according to Fig. 5. The primary controlling component of the SG is the Arduino Uno which connects a single-phase electric grid, a ZCD, an RTC module, esp8266, and an LCD [56].
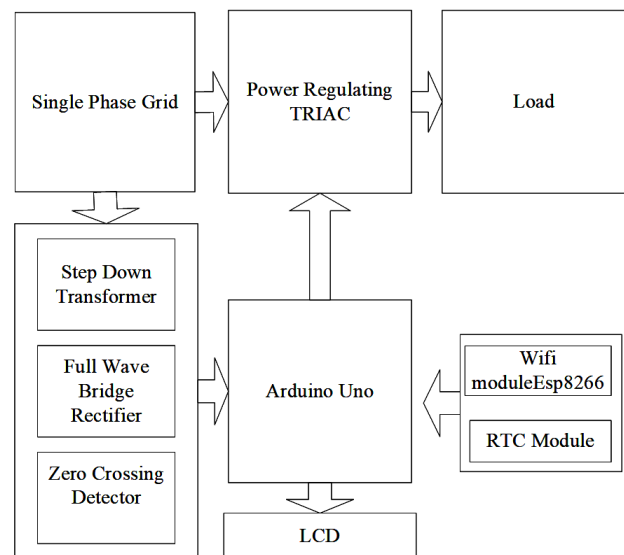

Fig. 4: Basic block diagram of the smart grid system.

A full-wave bridge rectifier (FWBR) is an electric circuit that converts *AC* to direct current (DC). The FWBR takes the 12 V *AC* output of the 220V single-phase *AC* step-down transformer. This 12V is fed to the FWBR diode that rectifies the 12 V *AC* to 12 V pulsating DC. This pulsating DC always goes to zero volt point every 10 milliseconds since the *AC* line frequency is 50 Hz. Fig. 6 makes it more understandable. The 12V *AC* line also changes phase in accordance with the phase change of 220 V AC. Therefore, the zero crossing points are the same for both signals. The pulsating DC of 12V is then fed to an optocoupler U4 (MOC3021) through a 250 Ω resistor to maintain the current limit. Another important aspect of the system is that it can automatically detect the voltage level of the grid through the voltage sensing section. The rectified and filtered voltage is fed into the Arduino through a variable resistor RV2 and then it is measured by
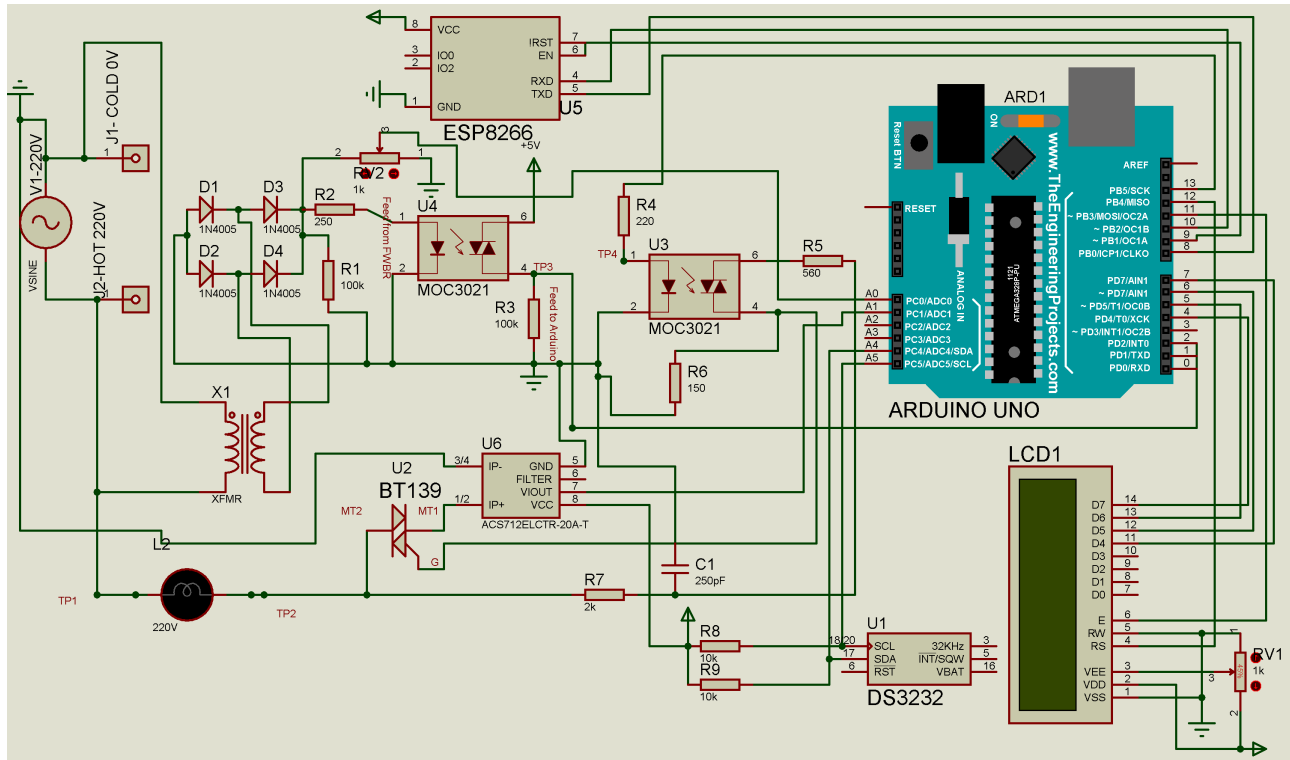
Fig. 5: Complete circuit diagram of the designed smart grid system.

analog port A0. ACS712 current sensor has also been introduced with Arduino to measure the current flow through the line. The V_{out} pin of the current sensor is connected to the analog port A1. Here, a stabilitron is employed to protect the circuit, which trips when the input voltage rises above 3.7V.

supplied to the optocoupler (Fig. 5). Thus, the optocoupler yields a falling edge of 5V to 0V and a rising edge of 0V to 5V across the resistor R3(100K) at the time of zero crossing of the 220V single-phase grid that has been displayed in Fig. 7. The Arduino Uno receives this rising edge at interrupt pin 2.
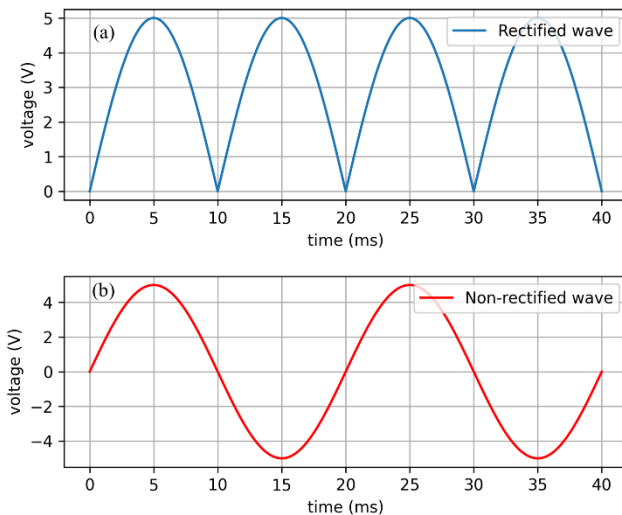

Fig. 6: (a) Rectified wave and (b) non-rectified wave output of ZCD.

Fig. 7: Arduino interrupts signal generation from ZCD: (a) Arduino interrupts signal, and (b) rectified output of 12V AC.

When the optocoupler input side is fed with zero voltage, it results in a non-conducting state at the output side of the optocoupler i.e., the optocoupler doesn't conduct. The non-conducting state at the output side of the optocoupler results in a voltage of 5V at pin 6 of U4 as 5V is being
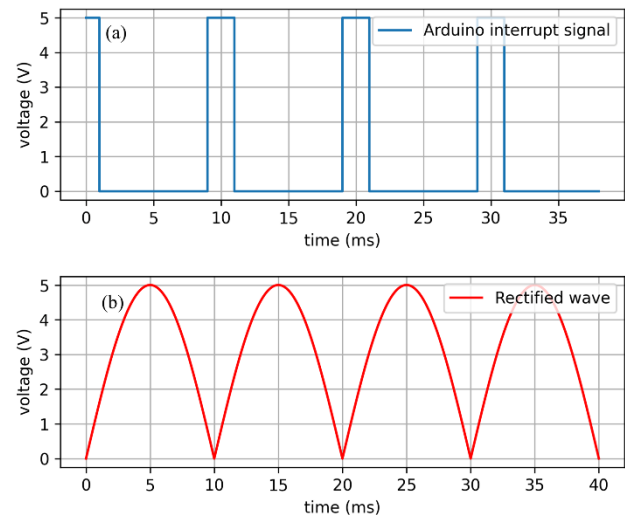
An interrupt routine is attached to Arduino pin 2 to execute the interrupt. A rising edge that comes from the optocoupler results in an interrupt to the Arduino Uno. If there is an Arduino Uno interrupt, it executes a routine that

contains Triggering logic and information to fire TRIAC. Triggering logic enables the Arduino digital pin 13 to a high state (Fig. 8). This output pin is connected with an optocoupler U3 through a 220Ω resistor (R4). When the output pin 13 is at a high state, optocoupler U3 goes to conducting state. Optocoupler U3 mainly isolates the microcontroller from the *AC* line voltage and also performs triggering of TRIAC. Optocoupler output side pin 6 is connected with the TRIAC main terminal 2 through a 560Ω resistor (R5) and pin 4 is connected to the ground through a 150Ω resistor (R6). The TRIAC gets the gate signal from the voltage developed across this R6 resistor. The TRIAC gate is also connected to the ground through a snubbing circuit (Fig. 5). This snubbing circuit is very crucial when the load is either inductive or capacitive. The snubbing circuit protects the TRIAC's gate from overvoltage spikes and the calculation of capacitance for the circuit is given in Equation (1) and Equation (2).

$$\frac{dV}{dt} = 50V/us \qquad (1)$$

$$\frac{dV}{dt} = \frac{.632Vs}{Rs * Cs} \qquad (2)$$

Where R_s is the series resistance, C_s is the series capacitance, and V_s is the voltage applied across C_s and R_s.
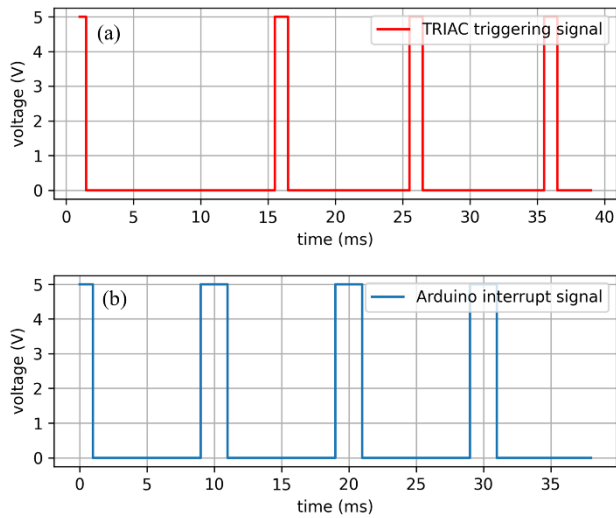

Fig. 8: Arduino interrupt and TRIAC triggering signal: (a) TRIAC triggering signal, and (b) Arduino interrupt signal.

The Arduino Uno gets the real timing information from the RTC (DS3232) module. The time of the clock is checked by Arduino Uno every five seconds. To interface the RTC module, SCL and SDA pin is connected with serial bus A5 and A4 of Arduino (Fig. 5). These two pins (A5, and A4) are pulled up to 5V through a 10k pull-up resistor. An RTC Arduino library is used to interface the DS3231 RTC module with Arduino.

According to Bangladesh Electricity Regulatory Commission (BERC) in general peak hour starts at 5 PM and end at 11 PM for all consumer category, 11 PM to 5 PM of the next day is considered an off-peak hour except for the Low Tension category [57]. This peak and off-peak schedule is applicable throughout the year in Bangladesh for all consumer categories. The RTC module notifies the peak hour of energy consumption to Arduino, and it fires the TRIAC with a delay that depends on the amount of energy that needs to be conserved.

In Bangladesh, a 50 Hz frequency signal is used that results in a period of 20 ms and 10 ms for half of the period. Delaying 2 ms creates a 60-degree firing angle of TRIAC as shown in Fig. 9, and an RMS output voltage with a 60-degree firing angle is calculated using equation (3) [58].

$$Vo = (Vm/\sqrt{2}\sqrt{(1 \div \pi)(\pi - \alpha + ((sin2\alpha \div 2))} \qquad (3)$$
$$\times 214$$

where V_o is the output voltage, V_m is the maximum voltage, and α is the TRIAC firing angle.
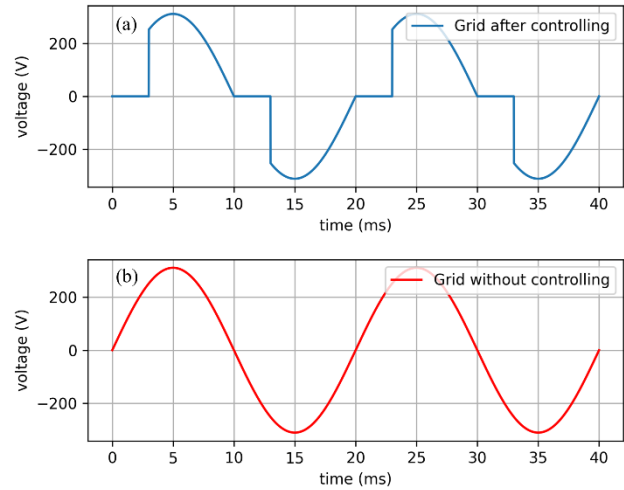

Fig. 9: Methodological grid: (a) with CVR technique, and (b) without CVR technique.

When the Arduino Uno board finds an off-peak hour, it fires the TRIAC without any delay and thus ensures the total voltage is supplied to the load without any modification. The instantaneous power and RMS voltage of a single-phase grid system can be calculated using equations (4) and (5) [59].

$$P = VI \qquad (4)$$

$$Vrms = \sqrt[2]{\frac{1}{10}\int_{t}^{10}(Vm \sin \omega t)^2 \, dt} \qquad (5)$$

Here t is the delayed time of triggering, P is the power, V_m is the maximum voltage, and V_{rms} is the RMS voltage.

Power conservation regarding TRIAC firing has been shown in Table 1. The table depicts that more delay in firing TRIAC results in more power saving.

Table 1. Methodologically conserved power (VA) at peak hours

Delay (ms)	Grid input (V)	Grid output (V)	Power conservation (%)
1	220	219.20	0.37
2	220	214.50	2.5
3	220	202.90	7.78

Since the voltage is lower than predicted, reactive power (given by capacitor) is required at that instant, or the other way around. Equation (6) depicts a simplified link between the voltage deviation at a particular place and the reactive power compensation requirements determined by the network's Thévénin Reactance [35].

$$|\Delta V| \approx \frac{|\Delta Q|}{X_{TH}} \tag{6}$$

where ΔV is the voltage deviation, ΔQ is the deviation of reactive power, and X_{TH} is the reactance

Arduino 1.6.5 is used to create and compile the program code that controls the system. The code is uploaded to the Arduino Uno board through a USB. Using the export compiled binary option found in the Arduino IDE's sketch menu, a hex file is produced to simulate the system on Proteus. . The pseudo-working procedure of the system is shown in the flowchart (Fig. 10).

3.4 Algorithm of the system

   i. Start the SG.
   ii. Connecting the system to the LAN using the SSID name and password of a nearby Wi-Fi network.
   iii. Check the grid voltage through the ZCD section.
   iv. Reading the current time (Current Time) and Peak hour (p_hour) from EEPROM location 1022.
   v. Is Current_Time == peak-hour (P_hour)?
   vi. Start power saving if it is a peak hour by delaying TRIAC firing by (2 ms - native delay by the system) in every interruption of ZCD; else fire the TRIAC without delay.
   vii. Displaying message of peak hour.
   viii. Read the current sensor.
   ix. Connect to the ThingSpeak cloud with API key
   x. Sending sensor data to ThingSpeak cloud for energy monitoring.
   xi. Repeating steps (d) to (j).

4. Results and discussion

4.1 Simulation results

The intended SG has been simulated using Proteus 8.9, Arduino 1.8, and python IDLE shell 3.9.6 on computer core i5. Arduino Uno, TRIAC load, optocoupler RTC
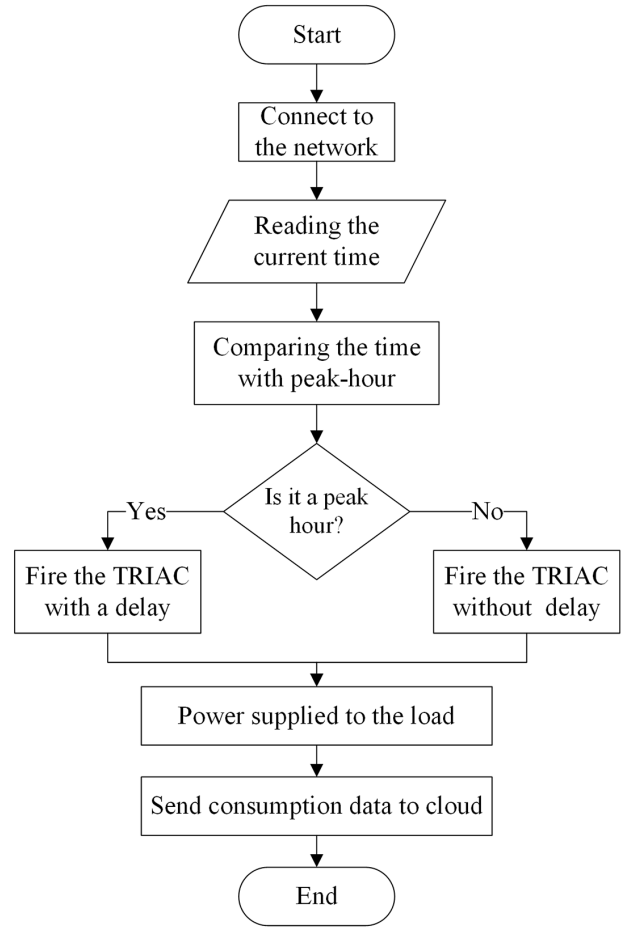

Fig. 10: Flowchart of the smart grid system.

module, and all the components were connected as shown in Fig. 5. The hex program file generated from Arduino IDE was imported to the Proteus Arduino part. Resistive (constant energy), constant current, and inductive (constant impedance) loads were connected within the SG to evaluate the performance. These loads yield different phenomena from each other while simulating with Proteus. To study the power supplying phenomena different power was supplied based on the schedule of peak and off-peak hours of the grid system.

Fig. 11 shows that there is no discrepancy in supplying power to the load. Switching TRIAC is smooth and no distortion was seen in supplying voltage by the smart grid in the Proteus simulation. The area between the red and blue lines is the power supplied to the load. The delay in firing the TRIAC was 3 ms during the simulation period. A 240 Ohm resistive load consumed 198 W power when there was no conditioning of the grid i.e., at the time of an off-peak hour, and consumed 167 W power at the time of peak hour (Fig. 11(b)).

A 75 Ohm constant impedance load is attached to the SG to study the capability test of the designed system. Despite the presence of a snubbing circuit, a voltage spike was observed at the time of TRIAC switching (Fig. 11(a)). This phenomenon can be explained by the elementary
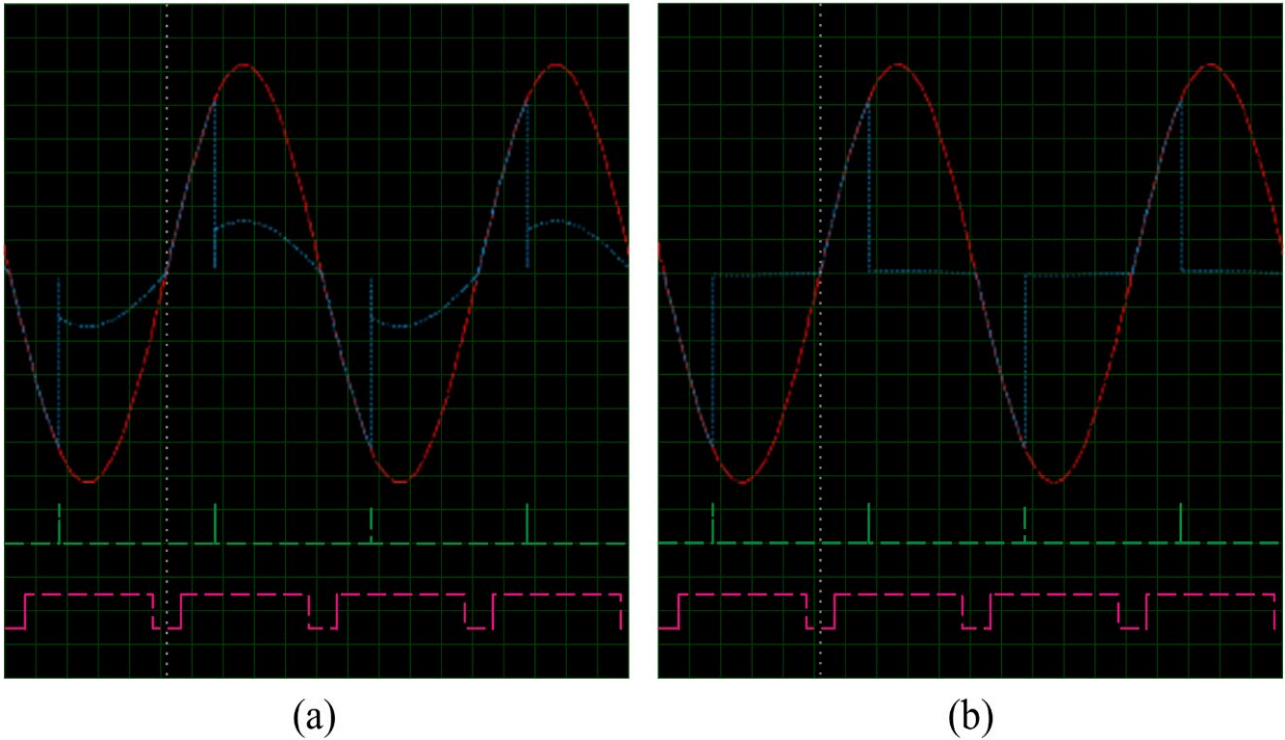
Fig. 11: Grid output voltage (channel A-red) along with interrupt and triggering signal: (a) Power supplied to a 70 Ohm inductive load, and (b) Power supplied to a resistive load during peak hours. The channel B (blue line) shows the TRIAC switched-off time. Channel C (magenta line) is the TRIAC triggering signal and channel D (green line) is the zero-cross detection signal. [Horizontal: s/div - 2ms; Vertical: channel A & B (V/div) - 50 V, channel C (V/div) - 5 V, channel D (V/div) - 1 V]

property of an inductive load which is the current change opposing property; due to the current change opposing properties of inductive load, TRIAC does not get the absolute turn-on condition i.e., there is always a voltage drop against the TRIAC at the time of powering the inductive load. During peak hours the constant impedance load consumes 50 W and 62 W at an off-peak hour. The power measurement was done by the wattmeter of Proteus 8.9. Moreover, the grid shows stable output on the consumer side.

4.2 Experimental results

Since the Arduino Uno board is used as the primary controlling unit, the performance of this appliance is enormously affected by the performance of Arduino Uno; i.e., the performance of Atmega328p which is the main microcontroller of this board. TRIAC also plays an important role in the performance of the system as this is a significant part of it. Another important thing that needs to be considered is the performance of the ZCD. If zero-crossing detection requires a large amount of time then the minimum firing angle will be increased. In the system, a MOC3021 optocoupler has been used that requires time to respond that also limits the performance of the system. Another part of this system is the TRIAC firing system which also requires time to respond. Accumulation of all the delays stated above makes a delay of 75.5 μs which is estimated by a simple algebraic sum of delays [TRIAC turn-on time (20 μs) + optocoupler turn-on time (2 μs) + Arduino instructions time (53.5 μs)] found from datasheets

[60–62]. Atmega328p takes 16 μs to execute an interrupt with a 16 MHz clock. ATmega328p requires 1-3 cycles per instruction. Inside the code, it was about 300 instructions. Considering 2 cycles on average per instruction, the total time for 300 instructions = (300*2)/16MHz = 37.5 μs. The native delay of the system is reduced by firing the TRIAC earlier. Gate-controlled turn-on time is 5 A/μs which further limits the system's performance. The performance of the zero-crossing detection meets the expectations (Fig. 12). It results in a peak on every zero crossing that interrupts the Arduino to fire the TRIAC.
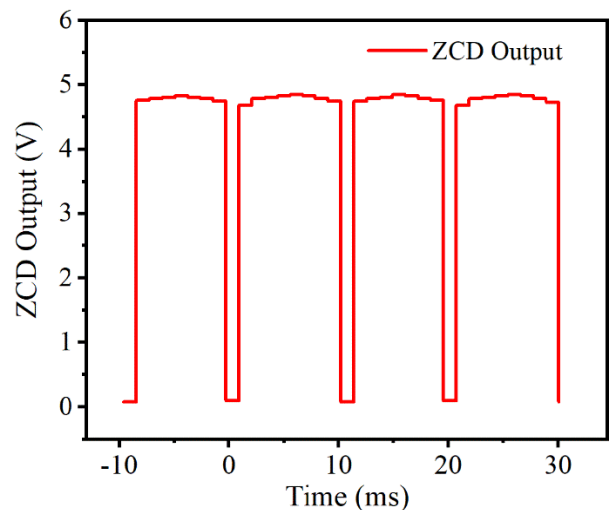

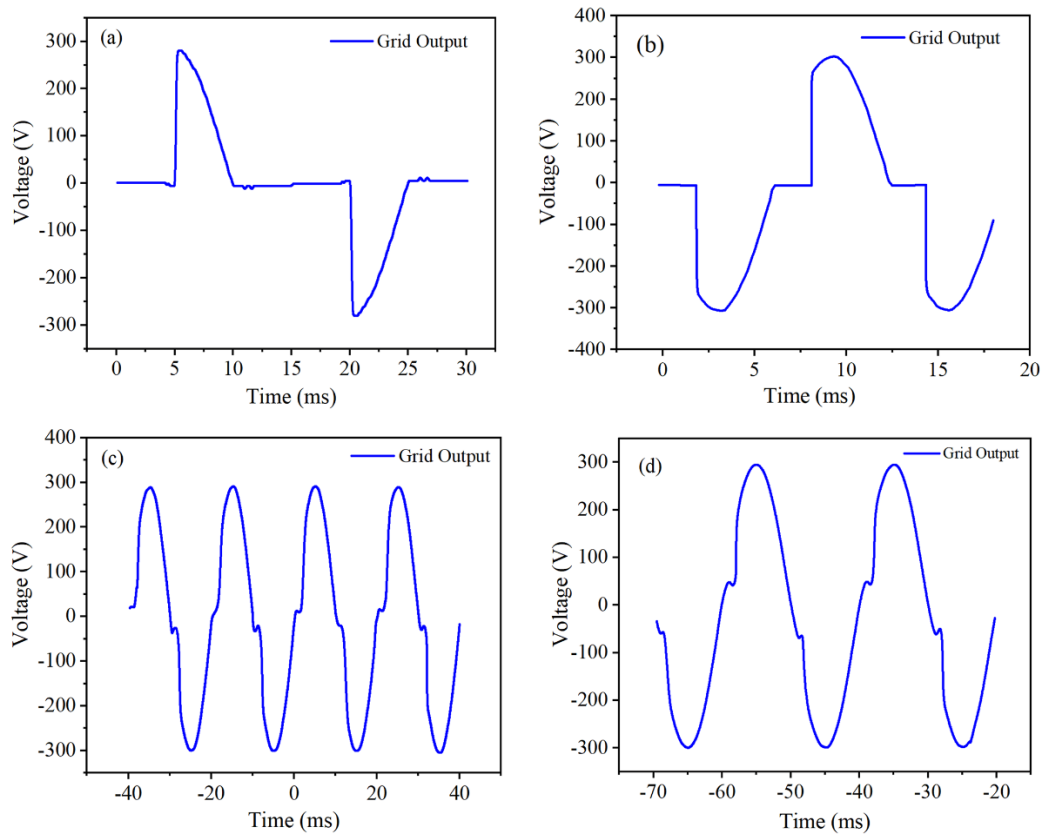**Fig. 12:** ZCD output captured in MS044 oscilloscope.

Fig. 13: Grid output voltage applying CVR technique: (a) Grid output voltage firing TRIAC 5 ms delay with resistive load, (b) grid output voltage firing TRIAC 3 ms delay with resistive load, (c) grid output voltage firing TRIAC 2 ms delay with constant impedance, and (d) grid output voltage firing TRIAC 2 ms delay with the constant impedance element.

In the developed system BT139 TRIAC has been used and its efficiency has been calculated through the proteus simulation tool. TRIAC efficiency is determined by the ratio of output power to input power. The power is measured by the wattmeter tool of proteus 8.9. For 480 Ω resistive load, its power is calculated and the input power was 100.3 VA, and the output power was 100 VA. From these two values, the efficiency of the TRIAC was determined as 99.7 %. According to the datasheet, its average gate power is 0.5 W but its maximum gate power is 5 W. The maximum holding current of the TRIAC is 45 mA where the gate triggering current is 0.1 A. On state RMS current of the TRIAC is 16 A [61]. In a practical scenario the efficiency of the TRIAC could be 97 to 98 % which is found by some researchers [42,63].

The system performance was checked by using a 100 W filament lamp bulb, 65 W ceiling fan, 2kW Philips water heater, 1.5 kW Vision water heater, 56 W Sony hi-speed mini fan, 20W superstar energy saving bulb, Samsung SyncMaster, and all other household electronics and electrical equipment to study the feasibility of the system. Here, the smart grid output voltage at the peak hour for the resistive load (constant energy) and inductive load (constant impedance load), are shown in Fig. 13 which are achieved by the MSO44 oscilloscope. Besides this, the impedance corresponding to the test load is measured using Agilent 4263 LCR meter which is shown in Table 2.

Table 2. Consumed power (VA) at peak hours by different test loads.

Type of load	Impedance (Ω)	Power consumed at 2 ms delayed condition (VA)
100 W lamp	480.26	81.852
56 W Hi-speed mini fan	562.93	49.91
2 kW Philips heater	24.263	1699.63
65 W Everest Ceiling fan	759.68	61.41
1.5 kW Vision heater	35.74	1136.87

4.3 Constant impedance load performance

Energy conservation using SG is about 8.83% considering a 2 ms firing delay. The performance of the constant impedance load is good except for some harmonics. Delaying more than 2 ms in firing TRIAC generates so many harmonics that it can't be considered for grid conditioning [64]. According to IEEE Standard 242-1986, harmonics tolerance of constant impedance load is moderate. Furthermore, the consumer also notices a loss of power as constant impedance load performance declines [65].

4.4 Constant energy load performance

The CVR factor for constant energy load is zero when the energy consumption duration is not fixed and it depends on the completion of tasks like boiling water for tea or coffee. In such cases, applications of CVR do not alter energy. However, it has been found that the technique is worthwhile for shifting the energy demand. In case of unchanged time, duration energy can be conserved and its conservation percentage is 5.66 which is lower than the constant impedance load.

It has been also found that harmonics were very low for constant energy load to the constant impedance load though harmonics tolerance for constant energy load is very high according to the IEEE protocol (IEEE Standard 242-1986).

Constant Energy load performed remarkably well and did not show any harmonics at the time of TRIAC on or off and this type of load utilizes the smart grid at its optimum at peak-hour demand management. However, after a 3 ms delay, the change in lamp intensity was noticeable, and the system energy savings should not be increased further. The consumed power at the optimized condition is shown in Table 2 at the peak hour. 20 W superstar *AC* tube lamp showed some flickering when a small width (2 us) of triggering signal was given to TRIAC. This issue was solved after triggering multiple times with the same width or with the width of 200 us.

The performance and results of the system are quite positive. The system showed promising results in conserving power at the peak hour. Power consumed by different loads after using the smart grid is the apparent power which is calculated by multiplying the voltage and current drawn by the load.

The optimum power consumption of the load is compromised to conserve power during peak hours. The output of the system is optimized to an acceptable level for the consumer. The performance is analyzed for different levels of power preservation with different loads. Exploiting Equation (4), (5) it is found that less than 1 ms delayed triggering to TRIAC is not providing a satisfactory level of power conservation, and 2 ms to up delayed triggering to TRIAC is not providing a satisfactory level of performance to the consumer. Moreover ANSI standard allows 5% variation of voltage i.e., 209 V to 231 V
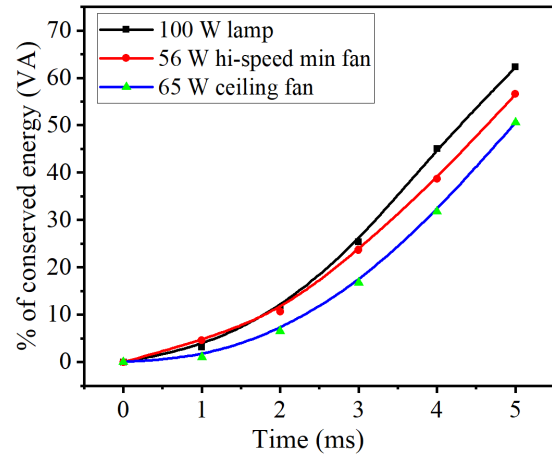

Fig. 14: Energy conserved for a different level of conditioning of the grid.

variation is acceptable [36]. The statistical result shows that a 1-2 ms delay in triggering conveys a substantial amount of energy conservation (Fig. 14) without troubling the consumer as well as satisfying the ANSI standard. From Fig. 14 and Table 2, it is evident that the power conservation percentage is bigger when the impedance of the load is smaller. In the case of a constant impedance load of 759.68 Ω, the energy conservation percentage is lower while the energy conservation percentage is significantly higher in the case of 562.93 Ω constant impedance load. The power consumption measurement of the 100 W Philips lamp is shown in Table 3. Table 3 denotes the power consumption after applying a delay in the system which has been measured using a standard power measuring tool. For the different amount of delays, the power consumption is different for different delays. More delay in firing TRIAC results in less power consumption and more power conservation. An important fact is different types of load result in different amounts of power conservation through their firing delay as well as impedance is the same. It might result from the combination of their internal elements. For instance, Table 3 shows 7.31 % power conservation for constant impedance load while the delay is 2 ms, though the average power conservation for constant impedance load is about 8.83 %.

Table 3. Methods were followed to measure power conservation for constant impedance load.

Time (ms)	Grid voltage (V)	Current (A)	Consumed power (VA)	Conserved power (VA)	% of conservation
0	224.7	0.41	92.13	**0.00**	**0.00**
1	222.9	0.40	89.16	**2.97**	**3.22**
2	215.4	0.38	81.85	**7.31**	**8.20**
3	202.2	0.34	68.75	**13.10**	**16.01**
4	180.9	0.28	50.65	**18.10**	**26.32**
5	151.1	0.23	34.75	**15.90**	**31.39**

A delay in TRIAC triggering for more than 3 ms results in a significant drop in the performance of devices like fans or lamps. It also does not meet the ANSI standard. Conserving energy with compromising performance is not desired by the consumer. It has been found via the trial-and-error approach that a firing delay of 2 ms is the best one for balancing performance and conservation. The main challenge in finding the effectiveness of CVR is the estimation of load [52,64,66–68]. Finally, the power consumption by the consumer is measured and sent to the ThingSpeak cloud for monitoring and analysis. The power consumption pattern of a consumer has been monitored on ThingSpeak and is shown in Fig. 15.
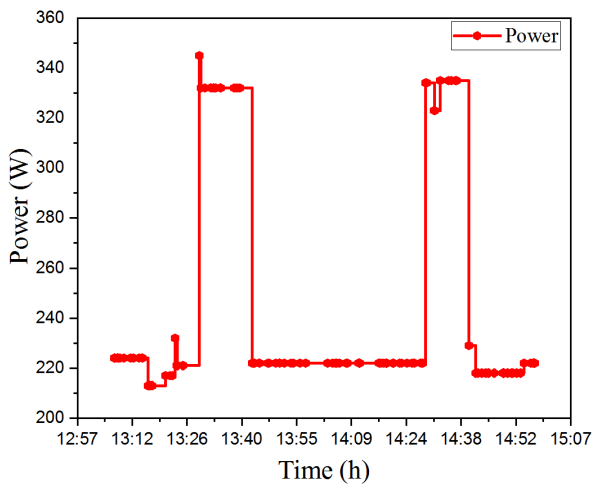

Fig. 15: Power consumption monitored on ThinSpeak cloud.

Furthermore, a protocol was created to turn off the power supply if the consumer consumes more than 3.30 kW. Field 1 power consumption plot of Channel ID (1935419) is tested by distribution end on every numeric insertion successfully. Every time power goes beyond 3.3 kW, SG cuts the power line along with a tweet saying "*You are consuming excess energy*" (Fig. 16).

Fig. 16: Notification through twitter.

Without knowing the load combination it's difficult to find the exact energy-saving efficiency [69] of the SG after implementing the CVR technique [70].

The developed system has a significant amount of load-shedding-reducing capabilities that cause by the power generation and demand gap at the peak hour. The system also can manage peak-hour load, which is an intriguing feature. This feature is becoming more and more important as time goes on because of the upward trend in the peak-to-average electricity demand ratio [59].

5. Conclusions

In this paper, an Arduino-based prototype of an SG was developed that conserves power by employing the CVR technique at peak hours. The peak hour was detected through an RTC module and the voltage level and phase were detected via the ZCD section. The peak hour as well as the voltage level was successfully identified by the system. At peak hour CVR technique was successfully applied through the system to conserve energy and the power conservation was calculated for the CVR factor equal to 1 considering 2 ms as the optimized firing delay. The system depicts the possibility of reducing up to 8.83% electricity consumption at peak hours. The SG is also connected to the ThingSpeak cloud and the power consumption pattern can be monitored and controlled from the distribution end. Consumers are also notified through tweets if they consume excessive power. The developed SG also cuts the power by monitoring the individual consumer power consumption. The efficacy of the system could be improved by understanding the unknown load composition in advance.

Nomenclature

AC	alternating current
AI	artificial intelligence
ANSI	American National Standard
BERC	Bangladesh Electricity Regulatory Commission
CVR	energy conservation by voltage reduction
CVR_f	conservation voltage reduction factor
DC	direct current
EMC	environmental modeling center
FWBR	full-wave bridge rectifier
IoT	Internet of things
LAN	local area network
LSTM	long short-term memory
LTV	load-to-voltage
ML	machine learning
MS-ABC	multi-swarm artificial bee colony
NN	neural network
NOAA	national oceanic and atmospheric administration
PLC	programmable logic controller
RTC	real-time clock
SCDA	supervisory control and data acquisition
SDP	stochastic dynamic programming

SG	smart grid
SN	sensor network
TRIAC	triode for AC
ZCD	zero-crossing detector
ZIP	impedance(Z), current(I), power(P)

Greek symbols

α	firing angle
ω	angular momentum
Ω	resistance

Conflicts of interest

The authors declare that they have no competing interests.

Acknowledgments

References

1) J.-C. Kim, S.-M. Cho, and H.-S. Shin, "Advanced power distribution system configuration for smart grid," *IEEE Trans. Smart Grid*, **4** (*1*) 353–358 (2013). doi:10.1109/TSG.2012.2233771.

2) Hoedi Prasetyo, "On-grid photovoltaic system power monitoring based on open source and low-cost internet of things platform," *Evergreen*, **8** (*1*) 98–106 (2021). doi:10.5109/4372265.

3) Siva Subrahmanyam Mendu, P. Appikonda, and Anil Kumar Emadabathuni, "Techno-economic comparative analysis between grid-connected and stand-alone integrated energy systems for an educational institute," *Evergreen*, **7** (*3*) 382–395 (2020). doi:10.5109/4068616.

4) M.K. Barai, and B.B. Saha, "Energy security and sustainability in japan," *Evergreen*, **2** (*1*) 49–56 (2015). doi:10.5109/1500427.

5) H. Han, M. Hatta, and H. Rahman, "Smart ventilation for energy conservation in buildings," *Evergreen*, **6** (*1*) 44–51 (2019). doi:10.5109/2321005.

6) M.K. Hossain, G.A. Raihan, M.A. Akbar, M.H. Kabir Rubel, M.H. Ahmed, M.I. Khan, S. Hossain, S.K. Sen, M.I.E. Jalal, and A. El-Denglawey, "Current applications and future potential of rare earth oxides in sustainable nuclear, radiation, and energy devices: a review," *ACS Appl. Electron. Mater.*, **4** (*7*) 3327–3353 (2022). doi:10.1021/acsaelm.2c00069.

7) M.K. Hossain, R. Chanda, A. El-Denglawey, T. Emrose, M.T. Rahman, M.C. Biswas, and K. Hashizume, "Recent progress in barium zirconate proton conductors for electrochemical hydrogen

device applications: a review," *Ceram. Int.*, **47** (*17*) 23725–23748 (2021). doi:10.1016/j.ceramint.2021.05.167.

8) K. Uddin, B.B. Saha, K. Thu, and S. Koyama, "Low GWP Refrigerants for Energy Conservation and Environmental Sustainability," in: 2019: pp. 485–517. doi:10.1007/978-981-13-3302-6_15.

9) M.K. Basher, M.K. Hossain, M.J. Uddin, M.A.R. Akand, and K.M. Shorowordi, "Effect of pyramidal texturization on the optical surface reflectance of monocrystalline photovoltaic silicon wafers," *Optik (Stuttg).*, **172** 801–811 (2018). doi:10.1016/j.ijleo.2018.07.116.

10) M.K. Basher, M.K. Hossain, R. Afaz, S. Tayyaba, M.A.R. Akand, M.T. Rahman, and N.M. Eman, "Study and investigation of phosphorus doping time on emitter region for contact resistance optimization of monocrystalline silicon solar cell," *Results Phys.*, **10** 205–211 (2018). doi:10.1016/j.rinp.2018.05.038.

11) T. Huq, H.C. Ong, B.T. Chew, K.Y. Leong, and S.N. Kazi, "Review on aqueous graphene nanoplatelet nanofluids: preparation, stability, thermophysical properties, and applications in heat exchangers and solar thermal collectors," *Appl. Therm. Eng.*, **210** 118342 (2022). doi:10.1016/j.applthermaleng.2022.118342.

12) Z. Ren, L. Wu, Y. Pang, W. Zhang, and R. Yang, "Strategies for effectively harvesting wind energy based on triboelectric nanogenerators," *Nano Energy*, **100** 107522 (2022). doi:10.1016/j.nanoen.2022.107522.

13) I. Ali, H. Sun, G. Tariq, H. Ali, K. Baz, H. Mahmood, I. Khan, and J. Yao, "Asymmetric impact of coal and gas on carbon dioxide emission in six asian countries: using asymmetric and non-linear approach," *J. Clean. Prod.*, **367** 132934 (2022). doi:10.1016/j.jclepro.2022.132934.

14) M.K. Hossain, K. Kawaguchi, and K. Hashizume, "Isotopic effect of proton conductivity in gadolinium sesquioxide," *Fusion Eng. Des.*, **171** 112555 (2021). doi:10.1016/j.fusengdes.2021.112555.

15) M.K. Hossain, M.C. Biswas, R.K. Chanda, M.H.K. Rubel, M.I. Khan, and K. Hashizume, "A review on experimental and theoretical studies of perovskite barium zirconate proton conductors," *Emergent Mater.*, **4** (*4*) 999–1027 (2021). doi:10.1007/s42247-021-00230-5.

16) M.K. Hossain, H. Tamura, and K. Hashizume, "Visualization of hydrogen isotope distribution in yttrium and cobalt doped barium zirconates," *J. Nucl. Mater.*, **538** 152207 (2020). doi:10.1016/j.jnucmat.2020.152207.

17) M.K. Hossain, K. Hashizume, S. Jo, K. Kawaguchi, and Y. Hatano, "Hydrogen isotope dissolution and release behavior of rare earth oxides," *Fusion Sci. Technol.*, **76** (*4*) 553–566 (2020). doi:10.1080/15361055.2020.1728173.

18) T. Ahmad, R. Madonski, D. Zhang, C. Huang, and A.

Mujeeb, "Data-driven probabilistic machine learning in sustainable smart energy/smart energy systems: key developments, challenges, and future research opportunities in the context of smart grid paradigm," *Renew. Sustain. Energy Rev.*, **160** 112128 (2022). doi:10.1016/j.rser.2022.112128.

19) M.Q. Raza, and A. Khosravi, "A review on artificial intelligence based load demand forecasting techniques for smart grid and buildings," *Renew. Sustain. Energy Rev.*, **50** 1352–1372 (2015). doi:10.1016/j.rser.2015.04.065.

20) J. Donadee, and M.D. Ilic, "Stochastic optimization of grid to vehicle frequency regulation capacity bids," *IEEE Trans. Smart Grid*, **5** (*2*) 1061–1069 (2014). doi:10.1109/TSG.2013.2290971.

21) F. Ahmad, A. Rasool, E. Ozsoy, R. Sekar, A. Sabanovic, and M. Elitaş, "Distribution system state estimation-a step towards smart grid," *Renew. Sustain. Energy Rev.*, **81** 2659–2671 (2018). doi:10.1016/j.rser.2017.06.071.

22) V. Vanitha, and E. Vallimurugan, "A hybrid approach for optimal energy management system of internet of things enabled residential buildings in smart grid," *Int. J. Energy Res.*, **46** (*9*) 12530–12548 (2022). doi:10.1002/er.8024.

23) B. Appasani, S.K. Mishra, A. V. Jha, S.K. Mishra, F.M. Enescu, I.S. Sorlei, F.G. Bîrleanu, N. Takorabet, P. Thounthong, and N. Bizon, "Blockchain-enabled smart grid applications: architecture, challenges, and solutions," *Sustainability*, **14** (*14*) 8801 (2022). doi:10.3390/su14148801.

24) V. Madhav Kuthadi, R. Selvaraj, S. Baskar, and P. Mohamed Shakeel, "Data security tolerance and portable based energy-efficient framework in sensor networks for smart grid environments," *Sustain. Energy Technol. Assessments*, **52** 102184 (2022). doi:10.1016/j.seta.2022.102184.

25) A. Kumar, M. Rizwan, and U. Nangia, "A hybrid optimization technique for proficient energy management in smart grid environment," *Int. J. Hydrogen Energy*, **47** (*8*) 5564–5576 (2022). doi:10.1016/j.ijhydene.2021.11.188.

26) M. Mohammadpourfard, A. Khalili, I. Genc, and C. Konstantinou, "Cyber-resilient smart cities: detection of malicious attacks in smart grids," *Sustain. Cities Soc.*, **75** 103116 (2021). doi:10.1016/j.scs.2021.103116.

27) K. Ma, X. Liu, G. Li, S. Hu, J. Yang, and X. Guan, "Resource allocation for smart grid communication based on a multi-swarm artificial bee colony algorithm with cooperative learning," *Eng. Appl. Artif. Intell.*, **81** 29–36 (2019). doi:10.1016/j.engappai.2018.12.002.

28) V.B. Pamshetti, S. Singh, A.K. Thakur, and S.P. Singh, "Multistage coordination volt/var control with cvr in active distribution network in presence of inverter-based dg units and soft open points," *IEEE Trans. Ind.*

Appl., **57** (*3*) 2035–2047 (2021). doi:10.1109/TIA.2021.3063667.

29) A. El-Shahat, R.J. Haddad, R. Alba-Flores, F. Rios, and Z. Helton, "Conservation voltage reduction case study," *IEEE Access*, **8** 55383–55397 (2020). doi:10.1109/ACCESS.2020.2981694.

30) J. Xu, B. Xie, S. Liao, Y. Sun, D. Ke, J. Yang, P. Li, L. Yu, Q. Xu, and X. Ma, "Online assessment of conservation voltage reduction effects with micro-perturbation," *IEEE Trans. Smart Grid*, **12** (*3*) 2224–2238 (2021). doi:10.1109/TSG.2020.3043957.

31) S. Jayaraman, M. Miranbeigi, R.P. Kandula, and D. Divan, "Improving energy efficiency and productivity at industrial plants using dynamic voltage management," *IEEE Trans. Ind. Appl.*, **56** (*2*) 1250–1257 (2020). doi:10.1109/TIA.2020.2965910.

32) K.R. Anjana, and R.S. Shaji, "A review on the features and technologies for energy efficiency of smart grid," *Int. J. Energy Res.*, **42** (*3*) 936–952 (2018). doi:10.1002/er.3852.

33) Z. Hu, C. Li, Y. Cao, B. Fang, L. He, and M. Zhang, "How smart grid contributes to energy sustainability," *Energy Procedia*, **61** 858–861 (2014). doi:10.1016/j.egypro.2014.11.982.

34) D. Kirshner, "Implementation of conservation voltage reduction at commonwealth edison," *IEEE Trans. Power Syst.*, **5** (*4*) 1178–1182 (1990). doi:10.1109/59.99368.

35) P.K. Sen, and K.H. Lee, "Conservation voltage reduction technique: an application guideline for smarter grid," *IEEE Trans. Ind. Appl.*, **52** (*3*) 2122–2128 (2016). doi:10.1109/TIA.2016.2525937.

36) "ANSI c84.1-2006 american national standard for electric power systems and equipment- voltage ratings(60 hertz)," (2006).

37) "Electric power monthly," *U.S. Energy Inf. Adm.*, (2012).
https://www.eia.gov/electricity/monthly/epm_table_grapher.php?t=table_5_03.

38) A. Farraj, E. Hammad, A. Al Daoud, and D. Kundur, "A game-theoretic analysis of cyber switching attacks and mitigation in smart grid systems," *IEEE Trans. Smart Grid*, **7** (*4*) 1846–1855 (2016). doi:10.1109/TSG.2015.2440095.

39) C. Clastres, "Smart grids: another step towards competition, energy security and climate change objectives," *Energy Policy*, **39** (*9*) 5399–5408 (2011). doi:10.1016/j.enpol.2011.05.024.

40) A. Abedi, L. Gaudard, and F. Romerio, "Review of major approaches to analyze vulnerability in power system," *Reliab. Eng. Syst. Saf.*, **183** 153–172 (2019). doi:10.1016/j.ress.2018.11.019.

41) D. Serrano-Jiménez, L. Abrahamsson, S. Castaño-Solís, and J. Sanz-Feito, "Electrical railway power supply systems: current situation and future trends," *Int. J. Electr. Power Energy Syst.*, **92** 181–192 (2017). doi:10.1016/j.ijepes.2017.05.008.

42) R.N. Anderson, A. Boulanger, W.B. Powell, and W. Scott, "Adaptive stochastic control for the smart grid," *Proc. IEEE*, **99** (*6*) 1098–1115 (2011). doi:10.1109/JPROC.2011.2109671.

43) F. Mohammadi, "Emerging challenges in smart grid cybersecurity enhancement: a review," *Energies*, **14** (*5*) 1380 (2021). doi:10.3390/en14051380.

44) D. Fan, Y. Ren, Q. Feng, Y. Liu, Z. Wang, and J. Lin, "Restoration of smart grids: current status, challenges, and opportunities," *Renew. Sustain. Energy Rev.*, **143** 110909 (2021). doi:10.1016/j.rser.2021.110909.

45) A. V. Jha, B. Appasani, A.N. Ghazali, P. Pattanayak, D.S. Gurjar, E. Kabalci, and D.K. Mohanta, "Smart grid cyber-physical systems: communication technologies, standards and challenges," *Wirel. Networks*, **27** (*4*) 2595–2613 (2021). doi:10.1007/s11276-021-02579-1.

46) F. Li, W. Qiao, H. Sun, H. Wan, J. Wang, Y. Xia, Z. Xu, and P. Zhang, "Smart transmission grid: vision and framework," *IEEE Trans. Smart Grid*, **1** (*2*) 168–177 (2010). doi:10.1109/TSG.2010.2053726.

47) K. Shahid, K. Nainar, R.L. Olsen, F. Iov, M. Lyhne, and G. Morgante, "On the use of common information model for smart grid applications — a conceptual approach," *IEEE Trans. Smart Grid*, **12** (*6*) 5060–5072 (2021). doi:10.1109/TSG.2021.3095896.

48) A.-H. Mohsenian-Rad, V.W.S. Wong, J. Jatskevich, R. Schober, and A. Leon-Garcia, "Autonomous demand-side management based on game-theoretic energy consumption scheduling for the future smart grid," *IEEE Trans. Smart Grid*, **1** (*3*) 320–331 (2010). doi:10.1109/TSG.2010.2089069.

49) W. Niu, F. Yang, and Y. Yuan, "Power Generation Scheduling for Long Distance Consumption of Wind-Solar-Thermal Power Based on Game-Theory," in: 2022 7th Asia Conf. Power Electr. Eng., IEEE, 2022: pp. 773–777. doi:10.1109/ACPEE53904.2022.9783976.

50) P. Palensky, and D. Dietrich, "Demand side management: demand response, intelligent energy systems, and smart loads," *IEEE Trans. Ind. Informatics*, **7** (*3*) 381–388 (2011). doi:10.1109/TII.2011.2158841.

51) M.I. Henderson, D. Novosel, and M.L. Crow, "Electric power grid modernization trends, challenges, and opportunities," *IEEE Technol. Trend Pap.*, 1–17 (2017).

52) B.R. Scalley, and D.G. Kasten, "The effects of distribution voltage reduction on power and energy consumption," *IEEE Trans. Educ.*, **24** (*3*) 210–216 (1981). doi:10.1109/TE.1981.4321493.

53) K.P. Schneider, J.C. Fuller, F.K. Tuffner, and R. Singh, "Evaluation of Conservation Voltage Reduction (CVR) on a National Level," Richland, WA (United States), WA (United States), 2010. doi:10.2172/990131.

54) S.P.S. Singh, and S.P.S. Singh, "Energy saving estimation in distribution network with smart grid-enabled cvr and solar pv inverter," *IET Gener. Transm. Distrib.*, **12** (*6*) 1346–1358 (2018). doi:10.1049/iet-gtd.2017.0973.

55) R.H. Fletcher, and A. Saeed, "Integrating engineering and economic analysis for conservation voltage reduction," in: IEEE Power Eng. Soc. Summer Meet., IEEE, 2002: pp. 725–730. doi:10.1109/PESS.2002.1043401.

56) L. Raju, A.A. Morais, and R.S. Milton, "Advanced Energy Management of a Micro-grid Using Arduino and Multi-agent System," in: Lect. Notes Electr. Eng., Springer Verlag, 2018: pp. 65–76. doi:10.1007/978-981-10-4852-4_6.

57) "Retail Electricty Tariff rate, 2020," Bangladesh Electricity Regulatory Commission, Dhaka, 2020.

58) Muhammad H. Rashid, "Power Electronics: Circuits, Devices, and Application," 3rd ed., Pearson Prentice Hall, 2004.

59) Y. Yang, and F. Blaabjerg, "A new power calculation method for single-phase grid-connected systems," in: 2013 IEEE Int. Symp. Ind. Electron., IEEE, 2013: pp. 1–6. doi:10.1109/ISIE.2013.6563684.

60) Atmel Corporation, "ATmega328P [DATASHEET]," San Jose, CA, USA, 2015.

61) Philips Semiconductors, "Triacs BT139 series [DATASHEET]," Japan, 1997.

62) Semiconductor Components Industrie, "MOC3010M [DATASHEET]," 2018.

63) S.J. Yun, Y.K. Yun, and Y.S. Kim, "A low flicker triac dimmable direct ac led driver for always-on led arrays," *IEEE Access*, **8** 198925–198934 (2020). doi:10.1109/ACCESS.2020.3034334.

64) M. Chen, R. Shoults, J. Fitzer, and H. Songster, "The effects of reduced voltages on the efficiency of electric loads," *IEEE Trans. Power Appar. Syst.*, **PAS-101** (*7*) 2158–2166 (1982). doi:10.1109/TPAS.1982.317486.

65) T.L. Wilson, "Measurement and verification of distribution voltage optimization results for the IEEE power & energy society," in: IEEE PES Gen. Meet., IEEE, 2010: pp. 1–9. doi:10.1109/PES.2010.5589762.

66) J. Erickson, and S. Gilligan, "The effects of voltage reduction on distribution circuit loads," *IEEE Trans. Power Appar. Syst.*, **PAS-101** (*7*) 2014–2018 (1982). doi:10.1109/TPAS.1982.317449.

67) W.G. Sunderman, "Conservation voltage reduction system modeling, measurement, and verification," in: PES T&D 2012, IEEE, 2012: pp. 1–4. doi:10.1109/TDC.2012.6281598.

68) Y. Yan, Y. Qian, H. Sharif, and D. Tipper, "A survey on smart grid communication infrastructures: motivations, requirements and challenges," *IEEE Commun. Surv. Tutorials*, **15** (*1*) 5–20 (2013). doi:10.1109/SURV.2012.021312.00034.

69) A. Bari, J. Jiang, W. Saad, and A. Jaekel, "Challenges in the smart grid applications: an overview," *Int. J.*

Distrib. Sens. Networks, **10** (*2*) 974682 (2014). doi:10.1155/2014/974682.

70) Z. Wang, and J. Wang, "Time-varying stochastic assessment of conservation voltage reduction based on load modeling," *IEEE Trans. Power Syst.*, **29** (*5*) 2321–2328 (2014). doi:10.1109/TPWRS.2014. 2304641.